Self-Assembly on Surfaces

DOI: 10.1002/anie.201300948

"Magic" Surface Clustering of Borazines Driven by Repulsive Intermolecular Forces**

Simon Kervyn, Nataliya Kalashnyk, Massimo Riello, Ben Moreton, Jonathan Tasseroul, Johan Wouters, Tim S. Jones, Alessandro De Vita, Giovanni Costantini,* and Davide Bonifazi**

Dedicated to Professor Maurizio Prato on the occasion of his 60th birthday

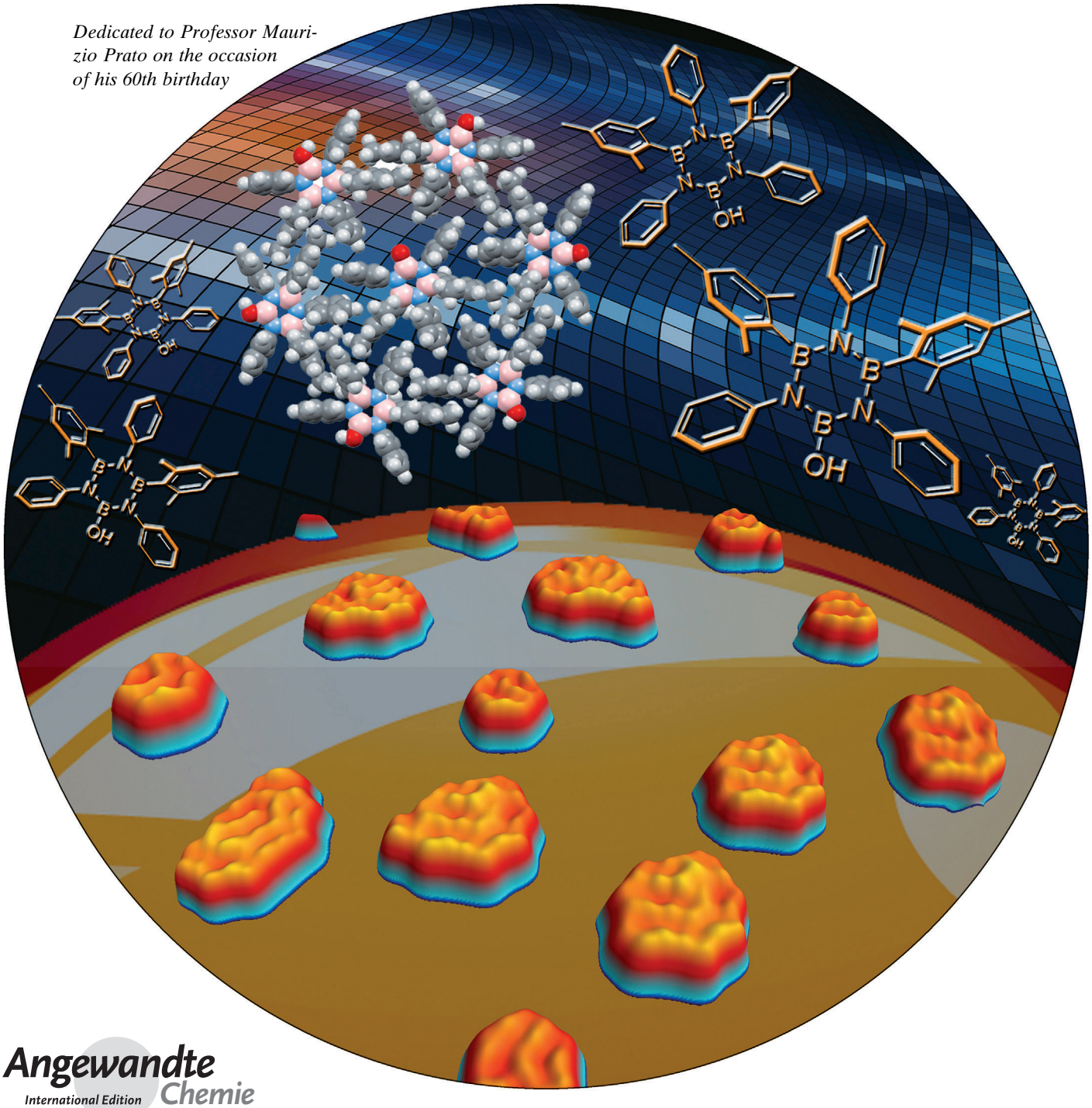

The different types of covalent bonds that carbon atoms can form yield a variety of fascinating structures with unique structural, chemical, and physical properties.[1] For example, discrete and extended polycyclic aromatic hydrocarbons (PAHs), such as graphene[2] or graphene nanoribbons[3] are emerging as novel, transformational molecular materials.[4] Replacing carbon by isostructural atoms is also emerging as a versatile functionalization strategy, for example, to tune optoelectronic and mechanical properties.[5] In particular, the substitution of C=C bonds by B–N covalent couples leads to isoelectronic molecular mimics bearing strong local dipole moments.[6] This polarity significantly affects the electronic properties[7] triggering the formation of self-assembled architectures.[8] In this respect, borazine ($B_3N_3H_3$) and its derivatives[9] have played a significant role as precursors for preparing bulk[10] and thin-layer[11] BN-based ceramics and ultrathin insulators,[12] and B-trimesityl-*N*-triphenylborazine derivative **1** was recently proposed as a viable active layer for optoelectronic devices.[13b] The study of borazine interactions on solid surfaces has to date been largely unexplored, although understanding and controlling the assembly of borazine molecular layers[14] could provide the conceptual basis to engineer functional supramolecular materials.

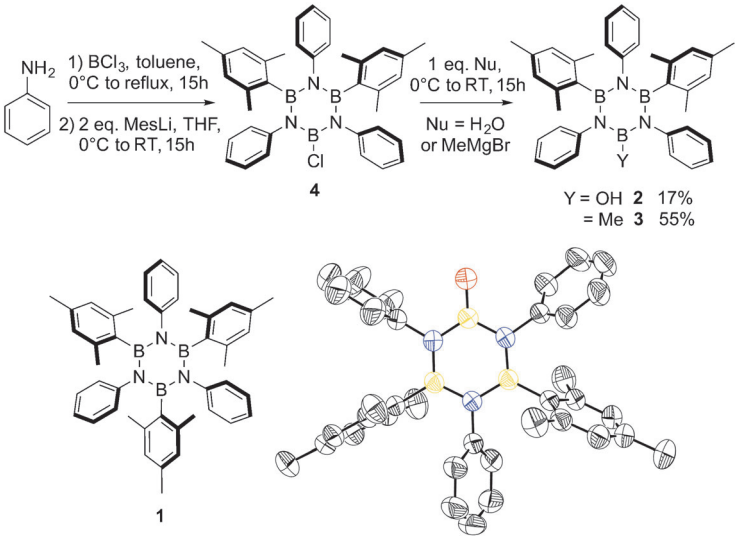

Scheme 1. Top: synthetic pathway for hydroxy- and methyl-bearing borazines **2** and **3**. Below: chemical formula of trimesityl borazine **1** and ORTEP representation of **2** as determined by X-ray diffraction analysis (blue N, red O, yellow B, gray C; atomic displacement parameters, obtained at 293 K, are set at the 50% probability level).

Herein, we report the first bottom-up preparation of borazine-based supramolecular architectures on a metal surface. We find that hexaaryl and hydroxypentaaryl borazine derivatives assemble in very different architectures on Cu(111) surfaces, as revealed by low-temperature (LT) scanning tunneling microscopy (STM) imaging. Whereas borazine **1** forms virtually faultless monolayers of interleaved monomeric units, hydroxypentaaryl borazine **2** yields exclusive formation of discrete "magic"[15] clusters.

Following the experimental routes developed for molecule **1**,[13b] **2** was obtained after reaction of aniline with BCl_3 upon subsequent addition of two equivalents of 2-mesitylllithium (MesLi) and one equivalent of water (Scheme 1).[13c] A small transparent crystal of borazine **2**, suitable for X-ray diffraction, was obtained by solvent evaporation (space group: $P2_1/c$) and confirms the presence of the acidic B–OH function.

The first step in the formation of the molecular layers is the thermal deposition of the borazine derivatives onto a room-temperature Cu(111) surface under ultrahigh vacuum (UHV). At any coverage, high-resolution low-temperature (77 K) STM images of borazine **1** acquired on Cu(111) reveal highly ordered islands (Figure 1) of molecules lying "flat" with the central borazine core parallel to the substrate. The individual molecules are imaged as groups of three lobes with a slightly distorted triangular shape (Figure 1c), where each lobe is attributable to a Mes group.[16]

[*] S. Kervyn,[+] J. Tasseroul, Prof. Dr. J. Wouters, Prof. Dr. D. Bonifazi
Department of Chemistry and Namur Research College (NARC), University of Namur (UNamur)
Rue de Bruxelles 61, Namur 5000 (Belgium)
E-mail: davide.bonifazi@fundp.ac.be
Prof. Dr. D. Bonifazi
Department of Pharmaceutical and Chemical Sciences and INSTM UdR Trieste; University of Trieste
Piazzale Europa 1, Trieste 34127 (Italy)
M. Riello,[+] Prof. Dr. A. De Vita
Physics Department, King's College London
London, WC2R 2LS (UK)
E-mail: alessandro.de_vita@kcl.ac.uk
Dr. N. Kalashnyk,[+] B. Moreton, Prof. Dr. T. S. Jones, Prof. Dr. G. Costantini
Department of Chemistry, University of Warwick
Gibbet Hill Road, Coventry, CV4 7AL (UK)
E-mail: g.costantini@warwick.ac.uk
[+] These authors contributed equally.

[**] D.B. gratefully acknowledges the EU through the ERC Starting Grant "COLORLANDS" project, the FRS-FNRS (FRFC contracts no. 2.4.550.09and MIS no. F.4.505.10.F), the "Loterie Nationale", the Science Policy Office of the Belgian Federal Government (BELSPO-IAP 7/05 project), the "TINTIN" ARC project (09/14-023), the MIUR through the FIRB "Futuro in Ricerca" ("SUPRACARBON", contract no. RBFR10DAK6) and the University of Namur (internal funding). S.K. thanks FRIA-FNRS and the University of Namur for his doctoral fellowships. J.T. thanks FRIA-FNRS for his doctoral fellowship. G.C., T.S.J., and A.D.V. thank the EPSRC for support of this work through the ULISSE grant (EP/G044864/1). G.C. also acknowledges financial support from The Royal Society through Grant no. RG100917 and from the Warwick-Santander Fund. Some of the equipment used in this research was obtained through Birmingham Science City: "Innovative Uses for Advanced Materials in the Modern World" with support from Advantage West Midlands and part funded by the European Regional Development Fund.
Supporting information for this article is available on the WWW under http://dx.doi.org/10.1002/anie.201300948.

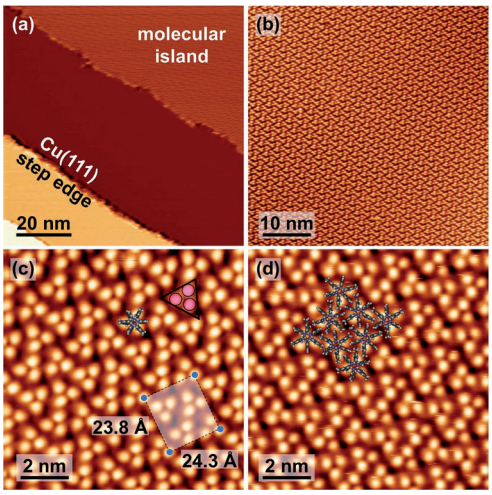

Figure 1. STM images for borazine **1** on Cu(111), deposited at 300 K, imaged at 77 K. a) Large area of the Cu(111) surface, top right: molecular island; bottom: bare Cu(111) surface. b)–c) Expanded views of the molecular islands; the three circles in the triangle in (c) correspond to the three Mes moieties; the shaded rectangle corresponds to the experimental unit cell. d) Calculated structure superimposed on the imaged monolayer.

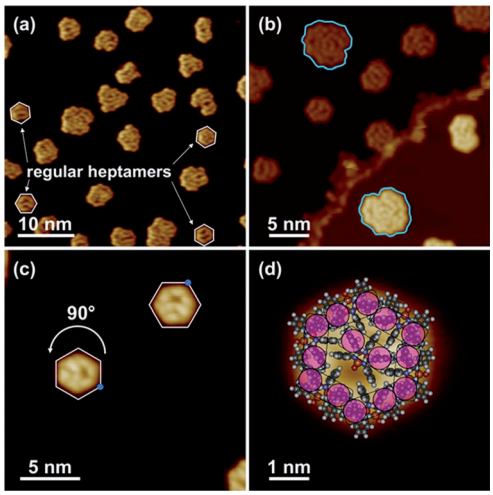

Figure 2. STM images of borazine **2** on Cu(111). a) Isolated molecular clusters, highlighting the regular 7-mers. b) Expanded view of a Cu(111) step edge, revealing two enantiomers of an irregular cluster. c) Expanded view of two 90°-rotated regular 7-mers. d) Calculated molecular model superimposed onto the 7-mer (purple circles correspond to the Mes moieties).

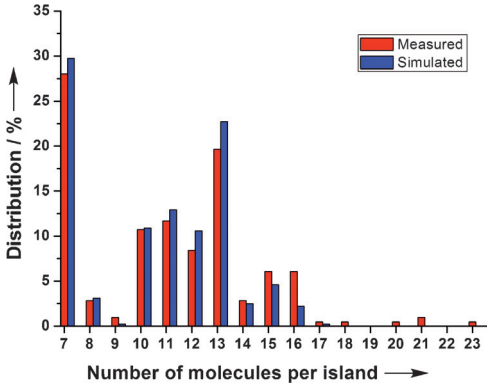

Figure 3. Experimental (red) and theoretical (blue) cluster size distribution of borazine **2**.

At variance with the standard surface-templated organization picture,[17] the absence of low-lying reactive molecular groups capable of directional interactions with the substrate is expected to induce low corrugation of the molecular adsorption potential. This situation suggests that the Cu(111) substrate plays a negligible role in the assembly. The assembly is instead driven by van der Waals (vdW) attractive forces through intermolecular interdigitation of the Mes and Ph rings of each molecule with those of its six nearest neighbors (Figure 1d). A Molecular Dynamics simulation of the system[18] for 2 ns at 250 K followed by cooling and equilibration at 77 K for 8 ns produced a stable interdigitated structure whose detailed features are in excellent agreement with the observed topography (Figure 1d).

In a second series of experiments, borazine **2** was sublimed on Cu(111) under the same submonolayer coverage conditions. Different from molecule **1**, hydroxy borazine **2** self-assembled into small isolated clusters in which each molecule appears as two aligned Mes lobes (Figure 2d). Clusters of different sizes were observed, composed of a minimum of 7 to a maximum of about 25 molecules (Figures 2a,b). The cluster shapes are well-defined and recurrent, although they do not generally correspond to regular geometries and appear as different isomers. A notable exception is the smallest observed cluster, hexagonal in shape and composed of six outer and one central borazine **2** (Figures 2c,d).

The observed cluster population shows distinct preferred "magic" peak values for clusters containing 7, 10, 11, 12, and 13 molecules (Figure 3). While the 7-mers and 13-mers occur with high frequency (28% and 20%, respectively), clusters bigger than the 13-mer are much less abundant, with the 14-mer being exceptionally rare. The interdigitation of aromatic substituents observed for borazine **1** is still present in all these clusters (Figure 2d). However, purely attractive short-range vdW forces cannot explain the observed formation of small clusters. A simple kinetic Monte Carlo (KMC) simulation using a discrete honeycomb lattice reveals that for any realistic vdW bonding strength, large molecular islands are the only possible assembly outcome in the relevant temperature/coverage range. This result suggests that repulsive interactions must also be present and determine the observed cluster distribution.

We analyzed our findings by means of a simple model where each molecule is allowed to bind with up to six neighbors, consistent with the general hexagonal shape of the B_3N_3 core (Supporting Information, Figure S8). This readily highlights the 7-mer as a first stable "magic" cluster in which all molecules have at least three molecular neighbors (Figure 2d). From here, the formation of an 8-mer and a 9-mer involves the iterated addition of a molecule bound to just two neighbors, which makes these clusters progressively less stable, consistent with the observations.

The 10-mer is the next expected "magic" number in which all molecules have at least three molecular neighbors (see also Figure S8 and text in the Supporting Information). We note that the acidic B–OH moiety in molecule **2** ($pK_a \approx 9$) can undergo deprotonation, leading to negatively charged adsorbed molecules, each effectively carrying a standing negative electrostatic dipole as result of the metal substrate (image–charge) screening. Deprotonation is expected to be promoted by polarization of neighboring molecules, screening the dipole formation.[19] Thus, borazine **2** molecules nested "inside" a cluster will be the most likely ones to undergo deprotonation. Any pair of electric dipoles associated with a couple of deprotonated molecules will however involve a repulsive long-range $1/r^3$ energy term, where r = distance between dipoles.

Indirect evidence of multiple deprotonation already occurring inside 10-mers (the smallest cluster with two non-perimeter molecules, Figure S8) is provided by STM images showing many different geometric isomers (Figure S5). This effect, consistent with the presence of repulsion forces within the cluster, is even more pronounced in the observed 11-mer and 12-mer population (Figure S6). The next in the series, the 13-mer cluster, is once more predicted to be distinctively stable, being the first "magic" cluster hosting two non-peripheral non-nearest-neighbor molecules able to undergo deprotonation while still only moderately repelling each other. This is consistent with the high observed occurrence of 13-mers (Figure 3).

The following 14-mer is the smallest cluster capable of decaying into two magic clusters. Such a process would be promoted by the repulsion between two charged molecules hosted in the 14-mer, which could explain the relatively rare occurrence of 14-mers and the high occurrence of 7-mers (Figure 3). Non-neighboring deprotonated molecule pairs could be accommodated in any cluster larger than the 14-mer. However, multiple deprotonations in large clusters would entail repulsions between many pairs of deprotonated molecules. This situation is expected to destabilize the large clusters for any fixed fraction of deprotonated molecules as the repelling pair number scales quadratically with cluster size. Consistently, we very rarely observe clusters larger than approximately 20 molecules.

These considerations were incorporated into a simple model Hamiltonian based on a discrete hexagonal lattice and including an attractive nearest-neighbor energy term and a repulsive $1/r^3$-scaling term (see Supporting Information). The rates associated with the cluster energies produced by this Hamiltonian were then used to predict the equilibrium cluster population, by means of a KMC simulation where cluster pairs exchange individual molecules, while 14-mers are allowed to occasionally split into two 7-mers. The distribution predicted by the model is reported in Figure 3 (blue histogram). The good agreement found confirms that the dipole-induced repulsion and the vdW attraction are the key parameters controlling the assembly in this system. This suggests that tuning their ratio in modified borazines of similar size could selectively promote 7-mers over larger clusters containing more than one deprotonated monomer. This is consistent with our model's predictions (see Supporting Information).

To check our conclusions and investigate possible molecular symmetry effects on the "magic" clustering process (assuming a conformation of the aryl rings perpendicular to the plane of the borazine ring, molecules **1** and **2** belong to the D_{3h} and C_{2v} point groups, respectively), we synthesized a reference, non-acidic methylpentaaryl borazine derivative **3** (point group: C_{2v}, see Scheme 1 and Supporting Information). Upon deposition on Cu(111), borazine **3** assembles into large islands similar to **1** (Figure S7), strongly supporting the conclusion that the "magic" cluster building of **2** is driven by long-range Coulomb repulsions arising from deprotonation reactions, as these reactions can occur in B–OH but not in B–CH_3.

In conclusion, we have demonstrated the first bottom-up preparation of borazine-based supramolecular architectures on a metal surface. Detailed STM studies show that molecule **1** self-organizes into large islands, whereas OH-bearing borazine **2** undergoes exclusive "magic" cluster building. These findings are rationalized as a delicate interplay of short-range vdW attractions between neighboring molecules and long-range Coulomb repulsions between deprotonated charged molecules. This picture is supported by theoretical modeling and further experiments on reference molecule **3** where deprotonation cannot occur and clustering is never observed. More generally, our theoretical model further suggests that the dipole strength and the vdW attraction between monomers could be independently varied in experiments designed to control the degree of monodispersion in the cluster size population.

Received: February 2, 2013
Revised: April 5, 2013
Published online: June 4, 2013

Keywords: borazine · scanning tunneling microscopy · self-assembly · supramolecular chemistry

[1] a) J. L. Delgado, M. Á. Herranz, N. Martin, *J. Mater. Chem.* **2008**, *18*, 1417–1426; b) L. Chen, Y. Hernandez, X. Feng, K. Müllen, *Angew. Chem.* **2012**, *124*, 7758–7773; *Angew. Chem. Int. Ed.* **2012**, *51*, 7640–7654.
[2] A. K. Geim, K. S. Novoselov, *Nat. Mater.* **2007**, *6*, 183–191.
[3] L. Dössel, L. Gherghel, X. Feng, K. Müllen, *Angew. Chem.* **2011**, *123*, 2588–2591; *Angew. Chem. Int. Ed.* **2011**, *50*, 2540–2543.
[4] a) F. Chen, N. J. Tao, *Acc. Chem. Res.* **2009**, *42*, 429–438; b) T. N. Hoheisel, S. Schrettl, R. Szilluweit, H. Frauenrath, *Angew. Chem.* **2010**, *122*, 6644–6664; *Angew. Chem. Int. Ed.* **2010**, *49*, 6496–6515.
[5] S. Kervyn, C. Aurisicchio, D. Bonifazi in *Functional Supramolecular Architectures for Organic Electronics and Nanotechnology* (Eds.: P. Samori, F. Cacialli), Wiley, Weinheim, **2010**; b) T. A. Schaub, M. Kivala *Arkivoc* **2013**, *i*, 175–184.
[6] a) Z. Q. Liu, T. B. Marder, *Angew. Chem.* **2008**, *120*, 248–250; *Angew. Chem. Int. Ed.* **2008**, *47*, 242–244; b) D. Golberg, Y. Bando, Y. Huang, T. Terao, M. Mitome, C. Tang, C. Zhi, *ACS Nano* **2010**, *4*, 2979–2993; c) K. Watanabe, T. Taniguchi, T. Niiyama, K. Miya, M. Taniguchi, *Nat. Photonics* **2009**, *3*, 591–594; d) K. Watanabe, T. Taniguchi, H. Kanda, *Nat. Mater.* **2004**, *3*, 404–409.

[7] a) A. J. V. Marwitz, A. N. Lamm, L. N. Zakharov, M. Vasiliu, D. A. Dixon, S.-Y. Liu, *Chem. Sci.* **2012**, *3*, 825 – 829; b) A. J. V. Marwitz, M. H. Matus, L. N. Zakharov, D. A. Dixon, S.-Y. Liu, *Angew. Chem.* **2009**, *121*, 991 – 995; *Angew. Chem. Int. Ed.* **2009**, *48*, 973 – 937; c) C. Zhi, Y. Bando, T. Terao, C. Tang, H. Kuwahara, D. Golberg, *Adv. Funct. Mater.* **2009**, *19*, 1857 – 1862; d) M. Côté, P. Haynes, C. Molteni, *Phys. Rev. B* **2001**, *63*, 125207.

[8] M. J. D. Bosdet, C. A. Jaska, W. E. Piers, T. S. Sorensen, M. Parvez, *Org. Lett.* **2007**, *9*, 1395 – 1398.

[9] a) A. Stock, E. Pohland, *Ber. Dtsch. Chem. Ges. B* **1926**, *59*, 2215 – 2223; b) S. J. Groszos, S. F. Stafiej, *J. Am. Chem. Soc.* **1958**, *80*, 1357 – 1360; c) A. Wakamiya, T. Ide, S. Yamaguchi, *J. Am. Chem. Soc.* **2005**, *127*, 14859 – 14866; d) J. Haberecht, R. Nesper, H. Grützmacher, *Chem. Mater.* **2005**, *17*, 2340 – 2347.

[10] a) J.-S. Li, C.-R. Zhang, B. Li, *Appl. Surf. Sci.* **2011**, *257*, 7752 – 7757; b) J. Li, S. Bernard, V. Salles, C. Gervais, P. Miele, *Chem. Mater.* **2010**, *22*, 2010 – 2019.

[11] L. Ci, L. Song, C. Jin, D. Jariwala, D. Wu, Y. Li, A. Srivastava, Z. F. Wang, K. Storr, L. Balicas et al., *Nat. Mater.* **2010**, *9*, 430 – 435.

[12] a) M. Corso, W. Auwärter, M. Muntwiler, A. Tamai, T. Greber, J. Osterwalder, *Science* **2004**, *303*, 217 – 220; b) J. Xue, J. Sanchez-Yamagishi, D. Bulmash, P. Jacquod, A. Deshpande, K. Watanabe, T. Taniguchi, P. Jarillo-Herrero, B. J. LeRoy, *Nat. Mater.* **2011**, *10*, 282 – 285.

[13] a) S. Kervyn, T. Nakanishi, J. Aimi, A. Saeki, S. Seki, B. Champagne, D. Bonifazi, *Chem. Lett.* **2012**, *41*, 1210 – 1212; b) S. Kervyn, O. Fenwick, F. Di Stasio, Y. Sig Shin, J. Wouters, G. Accorsi, S. Osella, D. Beljonne, F. Cacialli, D. Bonifazi, *Chem. Eur. J.* **2013**, *19*, 7771 – 7779; for the first report describing OH-functionalized borazines by-products see: c) S. Allaoud, B. Frange *Inorg. Chem.* **1985**, *24*, 2520 – 2523.

[14] a) J. V. Barth, G. Costantini, K. Kern, *Nature* **2005**, *437*, 671 – 679; b) J. A. A. W. Elemans, S. Lei, S. De Feyter, *Angew. Chem.* **2009**, *121*, 7434 – 7469; *Angew. Chem. Int. Ed.* **2009**, *48*, 7298 – 7333; c) D. Bonifazi, S. Mohnani, A. Llanes-Pallas, *Chem. Eur. J.* **2009**, *15*, 7004 – 7025; d) R. Otero, J. M. Gallego, A. L. Vázquez de Parga, N. Martín, R. Miranda, *Adv. Mater.* **2011**, *23*, 5148 – 5176.

[15] a) M. Böhringer, K. Morgenstern, W.-D. Schneider, R. Berndt, *J. Phys. Condens. Matter* **1999**, *11*, 9871 – 9878; b) A. D. Jewell, S. M. Simpson, A. Enders, E. Zurek, E. C. H. Sykes, *J. Phys. Chem. Lett.* **2012**, *3*, 2069 – 2075; c) C. Iacovita, P. Fesser, S. Vijayaraghavan, M. Enache, M. Stöhr, F. Diederich, T. Jung, *Chem. Eur. J.* **2012**, *18*, 14610 – 14613.

[16] a) F. Rosei, M. Schunack, P. Jiang, A. Gourdon, E. Lægsgaard, I. Stensgaard, C. Joachim, F. Besenbacher, *Science* **2002**, *296*, 328 – 331; b) L. Gross, K.-H. Rieder, F. Moresco, S. M. Stojkovic, A. Gourdon, C. Joachim, *Nat. Mater.* **2005**, *4*, 892 – 895.

[17] Selected examples: a) T. Classen, G. Fratesi, G. Costantini, S. Fabris, F. Louis Stadler, C. Kim, S. de Gironcoli, S. Baroni, K. Kern, *Angew. Chem.* **2005**, *117*, 6298 – 6301; *Angew. Chem. Int. Ed.* **2005**, *44*, 6142 – 6145; b) L.-A. Fendt, M. Stöhr, N. Wintjes, M. Enache, T. Jung, F. Diederich, *Chem. Eur. J.* **2009**, *15*, 11139 – 11150.

[18] An island composed of 36 molecules of borazine **1** placed on top of a four-layered metallic substrate slab yielding a (28.8 × 28.8 nm) surface unit cell, periodically repeated.

[19] J. B. Neaton, M. S. Hybertsen, S. G. Louie, *Phys. Rev. Lett.* **2006**, *97*, 216405.

